Chemical Science

EDGE ARTICLE

View Article Online
View Journal | View Issue



Cite this: *Chem. Sci.*, 2017, **8**, 298

# Pressure induced polymerization of acetylide anions in $CaC_2$ and $10^7$ fold enhancement of electrical conductivity†

Haiyan Zheng,‡[a] Lijuan Wang,‡[a] Kuo Li,*[ab] Youyou Yang,[c] Yajie Wang,[a] Jiajia Wu,[d] Xiao Dong,[a] Chun-Hai Wang,[e] Christopher A. Tulk,[f] Jamie J. Molaison,[f] Ilia N. Ivanov,[g] Mikhail Feygenson,[f] Wenge Yang,[abh] Malcolm Guthrie,§[b] Yusheng Zhao,[i] Ho-Kwang Mao[ab] and Changqing Jin[jk]

Transformation between different types of carbon–carbon bonding in carbides often results in a dramatic change of physical and chemical properties. Under external pressure, unsaturated carbon atoms form new covalent bonds regardless of the electrostatic repulsion. It was predicted that calcium acetylide (also known as calcium carbide, $CaC_2$) polymerizes to form calcium polyacetylide, calcium polyacenide and calcium graphenide under high pressure. In this work, the phase transitions of $CaC_2$ under external pressure were systematically investigated, and the amorphous phase was studied in detail for the first time. Polycarbide anions like $C_6^{6-}$ are identified with gas chromatography-mass spectrometry and several other techniques, which evidences the pressure induced polymerization of the acetylide anions and suggests the existence of the polyacenide fragment. Additionally, the process of polymerization is accompanied with a $10^7$ fold enhancement of the electrical conductivity. The polymerization of acetylide anions demonstrates that high pressure compression is a viable route to synthesize novel metal polycarbides and materials with extended carbon networks, while shedding light on the synthesis of more complicated metal organics.

Received 27th June 2016
Accepted 17th August 2016

DOI: 10.1039/c6sc02830f

www.rsc.org/chemicalscience

## Introduction

The metal carbide family is a large one containing several groups, including the materials based on extended 2D carbon structures, like the graphene-based Li-battery anode material $LiC_6$, and 0D ionic compounds like the $C_{60}$-based superconductor $K_3C_{60}$, acetylide-based salts $CaC_2$ and $Mg_2C$, as well as other groups. Their numerous intriguing physical and chemical properties are related to their structural peculiarities, which benefit from the rich chemistry of carbon. Compressing carbides to tens of gigapascals will facilitate the bonding between the isolated carbon groups, which will hence change the electrical properties significantly. For example, $BeC_2$ and $MgC_2$ are predicted to contain five-membered carbon rings,[1] and $Li_2C_2$ and $BaC_2$ are predicted to have polyanionic structures,[2,3] but only a few of these topics have been investigated experimentally.[3]

$CaC_2$ is the most important and common metal carbide used in industry. It is part of a large group of metal carbides that are composed of $M^{2+}$ and the dumbbell-shaped $C_2^{2-}$ anion. The polymorphs of $CaC_2$ have been studied for almost a century,[4–6] and four crystalline phases have been identified at ambient pressure, named $CaC_2$-I (space group (SG) $I4/mmm$); $CaC_2$-II (SG $C2/c$); $CaC_2$-III (SG $C2/m$); and $CaC_2$-IV (SG $Fm\bar{3}m$). All of these phases are composed of $Ca^{2+}$ and $C_2^{2-}$ in various configurations. Recently, several new polymorphs of $CaC_2$ stable under external pressure were predicted by theoretical researchers, with the $C_2^{2-}$ dumbbell-shaped anions connecting to one another to form carbon chains, graphene

[a]Center for High Pressure Science and Technology Advanced Research (HPSTAR), PO Box 8009, Beijing, 100088, China. E-mail: likuo@hpstar.ac.cn
[b]Geophysical Laboratory, Carnegie Institution of Washington, Washington DC, 20015, USA
[c]COFCO Nutrition & Health Research Institute, Beijing Key Laboratory of Nutrition Health and Food Safety, Beijing 100209, China
[d]Agilent Technologies (China) Co., Ltd., Wangjingbei Road, Chaoyang District, Beijing 100102, China
[e]Department of Chemistry, Durham University, South Road, Durham, DH1 3 LE, UK
[f]Spallation Neutron Source, Oak Ridge National Laboratory, Oak Ridge, TN 37830, USA
[g]Centre for Nanophase Materials Sciences, Oak Ridge National Laboratory, Oak Ridge, TN 37831, USA
[h]HPSynC, Geophysical Laboratory, Carnegie Institution of Washington, Argonne, IL 60439, USA
[i]Dept. of Physics, Southern University of Science and Technology, ShenZhen, China.
[j]Institute of Physics, Chinese Academy of Sciences, Beijing 100190, China
[k]Collaborative Innovation Centre of Quantum Matter, Beijing, China

† Electronic supplementary information (ESI) available: Details of GC-MS analysis. See DOI: 10.1039/c6sc02830f

‡ These authors contributed equally.

§ Present address: European Spallation Source ERIC, Lund, Sweden.

ribbons or sheets, which are actually Ca-graphenide, Ca-polyacenide and Ca-polyacetylide.[7–9] These polymorphs are expected to be metallic, and superconductive at low temperature.[7] However, up to now, experimental investigations of the high pressure transformation of $CaC_2$ have been subject to controversy. Two phase transitions were reported, with the first at 10–12 GPa, followed by an amorphization at a pressure above ~18 GPa.[10,11] Very recently, another report suggested the existence of the predicted *Cmcm* phase (Ca polyacetylide) above 7 GPa, and confirmed the amorphization upon further compression again.[12] The amorphization hindered almost all further investigations. In this work, we experimentally probed both the crystallized phases before the amorphization and the amorphous phase using several cutting-edge techniques, and evidenced the existence of linear and cyclic polycarbide anions in the product of the pressure induced polymerization of $CaC_2$.

## Results and discussion

### Variation of crystal structure

To investigate the phase transitions under high pressure, multiple *in situ* techniques including high pressure X-ray diffraction (XRD), neutron diffraction and Raman spectroscopy were employed. The lattice parameters of $CaC_2$-I under high pressure were determined by *in situ* XRD. In similarity to previous reports,[10,11] $CaC_2$ starts to amorphize above 18–20 GPa, above which the XRD peaks start to broaden and become indistinguishable. The unit cell parameters of $CaC_2$ under external pressure were determined by Rietveld refinement (Fig. 1). The reported phase transition at 10–12 GPa is too subtle to be confirmed in the plot of the pressure dependent lattice parameters, and the lattice parameter of the whole pressure range before amorphization can be fitted to a 3rd order Birch–Murnaghan (B–M) Equation of State (EOS), with $V_0 = 96.7(2)$ Å$^3$, $B_0 = 62(2)$ GPa, and $B_1 = 3.6(2)$.

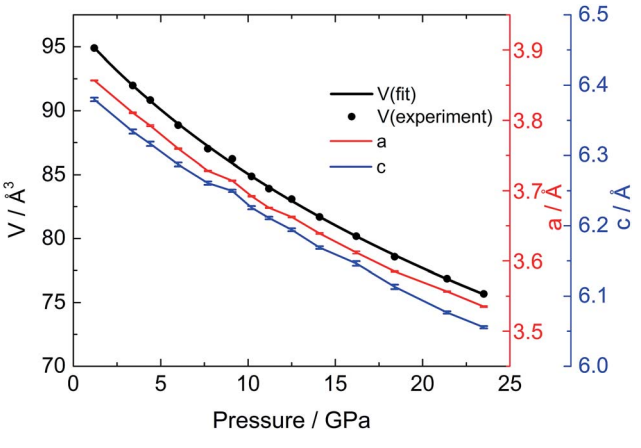


Fig. 1 Lattice parameters of $CaC_2$ under high pressure. The red and blue markers including error bars are for the *a* and *c*-axis respectively, and the lines are a guide for the eyes. The black dots are the experimental data of the unit cell volume, and the black solid line is the fitting of the BM-EOS.

To understand the structural details of $CaC_2$ under high pressure, *in situ* neutron diffraction was carried out (Fig. 2a), which is more sensitive to the positions of carbon atoms. The diffraction patterns below 10 GPa can be well fitted using the $CaC_2$-I structural model. The refined results are shown in Table S1† and a selected plot of Rietveld refinement is shown in Fig. S1.† However, above 10–12 GPa, the *hkl* peaks with $l \neq 0$ are significantly broadened, the C≡C bond length decreases significantly to unreasonable values and the nearest C···C intergroup distances increase correspondingly (Fig. 2b). This indicates that the $CaC_2$-I model is not suitable for the data above 10–12 GPa, though the averaged structure does not deviate from $CaC_2$-I dramatically. The reason for peak broadening comes from strain or disordering, most likely in the substructure of C instead of Ca, because the broadening is more pronounced in neutron diffraction.

The anomaly at 10–12 GPa was also found in the impedance spectrum, which will be discussed later. This can probably be attributed to the instability and interruption of the $CaC_2$-I lattice, because $CaC_2$-VI is more stable at this pressure, as predicted by theoretical investigations.[7,8,10] Our Density Functional Theory (DFT) calculations also show that $CaC_2$-VI is more stable than $CaC_2$-I above 9 GPa (Table S2†). As shown in Fig. 3, $CaC_2$-VI (Fig. 3b) is a distortion of $CaC_2$-I (Fig. 3a), with $\beta$ deviating from 90° and its space group *I*2/*m* being a subgroup of *I*4/*mmm*. Because no characteristic peak of $CaC_2$-VI can be identified under current experimental conditions, it seems the I–VI phase transition did not really go through, and the sample still stays in an intermediate state, like that shown in Fig. 3c. In this state, $CaC_2$-I is unstable; the phase transition starts locally (local disordering), but the new phase is not crystallized and cannot be identified.

### Spectroscopic investigation

To probe the functional groups, Raman spectroscopy was employed to detect the transition of the carbon–carbon bonds. In similarity to the reported results,[10] both the C–C stretching and $C_2$ libration modes show minor alterations at 10–12 GPa (Fig. 4a), which corresponds to the transition uncovered by the neutron diffraction experiment. Above 18–20 GPa, the Raman peaks start to degrade and disappear into the background, corresponding to the amorphization (Fig. S2†). After being maintained at ~30 GPa for 2 days, a minor peak at 1839 cm$^{-1}$ was observed, which is significantly lower than the C≡C stretching of $CaC_2$ before its disappearance (1916 cm$^{-1}$, Fig. 4b). When decompressed, the peak becomes more obvious and splits to two peaks at 1690 and 1850 cm$^{-1}$ (3.9 GPa) respectively. Such a peak should be attributed to an intermediate (or conjugated) state between a triple bond and a double bond, because its Raman shift is located between typical values for those bonds. The peak at 1850 cm$^{-1}$ is still around the region of triple bonds, while the peak at 1690 cm$^{-1}$ is approaching the region of double bond. This splitting provides further evidence that the peak at 1839 cm$^{-1}$ (before splitting) is from polymerized (oligomerized) carbon anions created by high

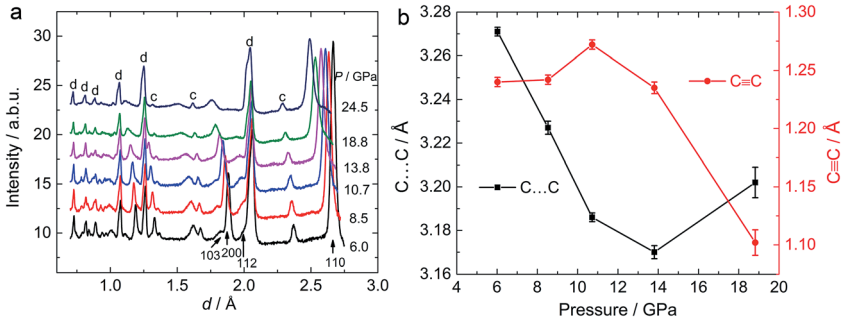


Fig. 2 *In situ* neutron diffraction patterns of $CaC_2$ under different values of pressure. (a) Neutron diffraction patterns of $CaC_2$ under high pressure. The peaks of diamond anvils and CaO are marked by d and c respectively. (b) C–C bond length and the nearest C···C distance between neighbouring $C_2^{2-}$ units under different values of external pressure.

pressure. Its decomposition at low pressure results in isolated triple bonds and other complex containing double bonds.

*In situ* infrared spectra were also measured to detect the vibration of carbon species (Fig. 5). The C–C stretching of the acetylide anion is symmetrical and is hence infrared inactive. This is why no absorption peak was observed at low pressure (up to ~21 GPa). Above 22 GPa, absorption peaks around 1750 $cm^{-1}$ and 1200 $cm^{-1}$ are observed. These peaks are in the range of the stretching modes of C=C double bonds and C–C single bonds. The bonds have to be asymmetric as they are infrared active, which means the carbon atom has at least two neighbours covalently bonded, and hence evidences the bonding between $C_2^{2-}$.

## Identification of polycarbide anions in the recovered sample

From the crystallographic and spectroscopic analysis, we conclude that the polymerization of acetylide anions happens in the amorphous state. The polycarbide anions would hence hide in the amorphous phase. Besides the spectroscopic investigations, neutron pair distribution function (PDF) analysis is employed to investigate the local structure of the amorphous phase, which gives the likelihood of finding an atom at a given radius from another atom at an arbitrary origin.[13] Obtaining good *in situ* PDF data above 20 GPa for $CaC_2$ is very challenging, if not impossible, therefore samples recovered from external pressure were measured (Fig. S3a†). No other periodic phase was identified from the recovered samples except $CaC_2$ (phase I, starting material). However, a distinct difference was found at the C≡C triple bond distance ($d \sim 1.24$ Å). The peak of the sample recovered from ~28 GPa is shifted to a greater radial distance and shows evidence for enhanced density between 1.3 Å and 1.5 Å when compared to that recovered from below 24 GPa (Fig. 6, more patterns in Fig. S3†). This verifies the presence of longer carbon–carbon bonds (C=C bonds) in the sample recovered from the highest pressure, which would be the product of the addition reaction between $C_2^{2-}$ ions.

More solid evidence comes from the Gas Chromatography-Mass Spectrometry (GC-MS) analysis. The hydrolysis of the polymerized $C_m^{x-}$ (here, $x$ is supposed to be equal to $m$) anions in the recovered sample will produce $C_{2n}H_{2n}$ ($Ca_nC_{2n} + 2nH_2O = nCa(OH)_2 + C_{2n}H_{2n}\uparrow$). In the hydrolyzed products, several tens of hydrocarbons were identified by GC-MS, which were not detected in the raw material (Fig. 7). It is worthy to point out that even with sub-microgram amounts of sample synthesized using a diamond anvil cell (DAC), similar results were obtained to those with a milligram amount of sample synthesized using a Paris-Edinburgh (PE) cell. This approach demonstrates that GC-MS has a significant application in the characterization of chemical reactions under extremely high pressure.

With the data obtained from the high-resolution quadrupole-time- of -flight-mass spectrometer (QTOF-MS), the molecular formulas of most peaks in the total ion chromatograms (TIC) can be determined unambiguously, as listed in Table S3.† These include $C_3H_4$, $C_5H_6$, $C_5H_4$, $C_6H_8$, $C_6H_6$, $C_6H_4$, and $C_8H_7$ in

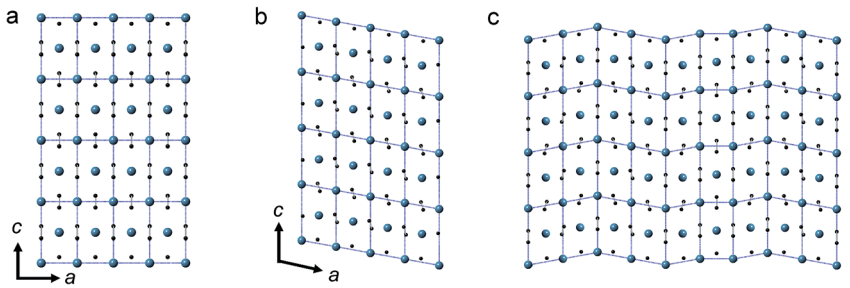


Fig. 3 Structures of $CaC_2$-I (a) and VI (b) viewed along [010]; (c) a schematic model of possible local disordering of $CaC_2$ above 12 GPa. The black spheres are for carbon atoms and the blue spheres are for calcium atoms.

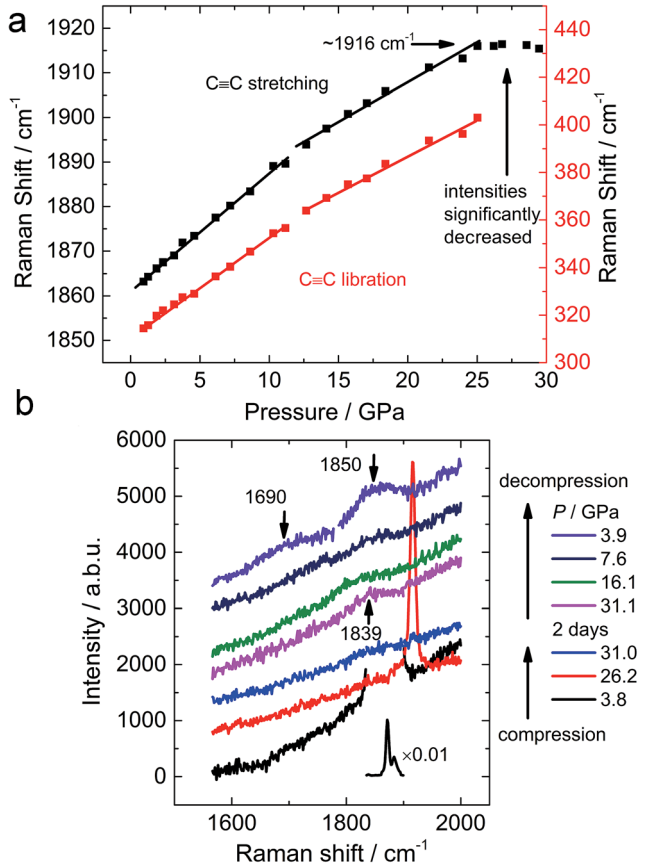


Fig. 4 (a) Pressure dependence of Raman shifts of $CaC_2$ and (b) selected Raman spectra of $CaC_2$ upon compression and decompression.

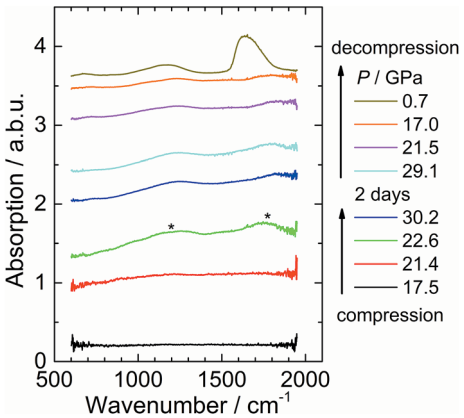


Fig. 5 Infrared absorption spectra of $CaC_2$ under external pressure.

the gas phase, with various numbers of isomers. More complicated molecules like $C_{12}H_{12}$, $C_{12}H_{10}$ and $C_{12}H_{14}$ can be identified in the liquid phase (Fig. S4 and Table S4†), and their diversities will be discussed in a following paper. All the identified molecules have a C : H ratio around 1 : 1, in consistency with the valence of carbon in $CaC_2$. The slight deviations from 1 : 1 probably result from the heterolytic cleavage of some unstable molecules or anions after or during the hydrolysis. The molecules with odd numbers of carbon atoms like $C_3H_4$ and $C_5H_4$ also likely result from cleavage, because the combination of $C_2^{2-}$ anions can only result in molecules with even numbers of carbon atoms. Hydrocarbons like $C_2H_6$, $C_2H_4$, $C_4H_8$ and those with a C : H molar ratio severely deviating from 1 : 1 are not detected, which excludes the existence of $C_2^{6-}$, $C_2^{4-}$, $C_4^{8-}$ and the corresponding calcium carbide. This indicates that the non-ox/red polymerization (or oligomerization) instead of disproportionation (or other ox/red reactions) dominates the reaction process, and the Ca : C molar ratio does not really change during the reaction.

By checking the corresponding mass spectrum in the National Institute of Standards and Technology (NIST) library, the peaks in the TIC are recognized. The list of possible molecules includes both linear and cyclic molecules, which result from the hydrolysis of linear and cyclic polycarbide anions respectively. By comparing the retention times, benzene can be identified unambiguously (Fig. S5 and S6†) among the peaks, which indicates the formation of $C_6^{6-}$ cyclic structures in the recovered $CaC_2$. It was predicted that carbon atoms tend to polymerize following the sequence of chain, belt and sheet, with increasing pressure. Both of the latter two structures (Ca polyacenide and Ca graphenide) contain six-membered rings.[7] Our experiment evidenced that under the current experimental conditions it is possible for $C_2^{2-}$ to polymerize to polyacenide (*Immm* phase in ref. 7) or its fragment, which was predicted to be stabilized above ~15 GPa. The chain structures can also exist due to incomplete reactions.

Calibrated by the working curve, the molar ratio of benzene to acetylene in the hydrolysis product is ~0.005 : 1 (Fig. S7†). Even if supposing other produced molecules respond at the same efficiency as benzene in MS (usually lower, thus the actual concentration is higher), the molar ratio of product to acetylene is 0.11 : 1. This indicates that a significant amount of $C_2^{2-}$ is reacted under the current experimental conditions. The details of the quantitative analysis are discussed in the ESI.†

## Meta-dynamic simulation

To build up a model to understand what happens in $CaC_2$ under external pressure, meta-dynamic simulations were performed at 30 GPa and two models were obtained (referred as to chain and ribbon models, shown in Fig. 8). In the chain structure, the acetylide anions are connected to form polyacetylide chains. Both *cis*- and *trans*- connections are formed, and branched chains are also obtained. Starting from this structure, a meta-dynamic simulation was conducted again and the ribbon structure was obtained, which is constructed by edge-sharing six-membered rings. These two models show the structural features of the sample under pressure and are consistent with the theoretical predictions in ref. 7, though with some defects. These two models are closely related. In the chain model, six-membered rings are identified and in the ring model, chains still exist. The co-existence of ring and chains is most likely the real case, as evidenced by the GC-MS experiment. It is worthy to note that the simulation is carried out using a box containing 64 Ca and 128 C atoms, constrained by

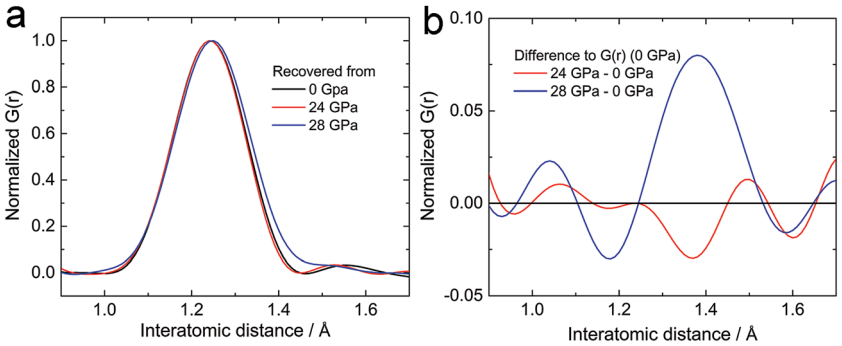


Fig. 6 Neutron pair distribution functions ($G(r)$) of $CaC_2$ samples recovered from external pressures. (a) Selected normalized first peak after background subtraction. This peak corresponds to the carbon–carbon bond. (b) Differences between the normalized $G(r)$ patterns of the samples recovered from high pressure (24 GPa, 28 GPa) and that of the raw material (0 GPa).

periodic boundary conditions. It can be anticipated that in the experiment the local structure will be more diverse, and it would be difficult for the produced covalent carbon network to crystallize.

This diversity uncovered by the simulation and experiment actually traced the whole process of polymerization, from small species to big ones, from chains to rings and ribbons. This is most likely what happened in the amorphous phase. The monomers polymerize with various degrees of polymerization and even in various dimensions. If the selectivity of the reaction is enhanced by controlling reaction conditions, more complex and kinetically stable metal carbides on milligram scales can be obtained besides the predicted phases.[7] Because the calcium polycarbide obtained is nucleophilic and highly reactive, more unexpected compounds can be synthesized through reaction with acid or *via* other nucleophilic reactions. The neutral molecules can even be separated by chromatography and purified.

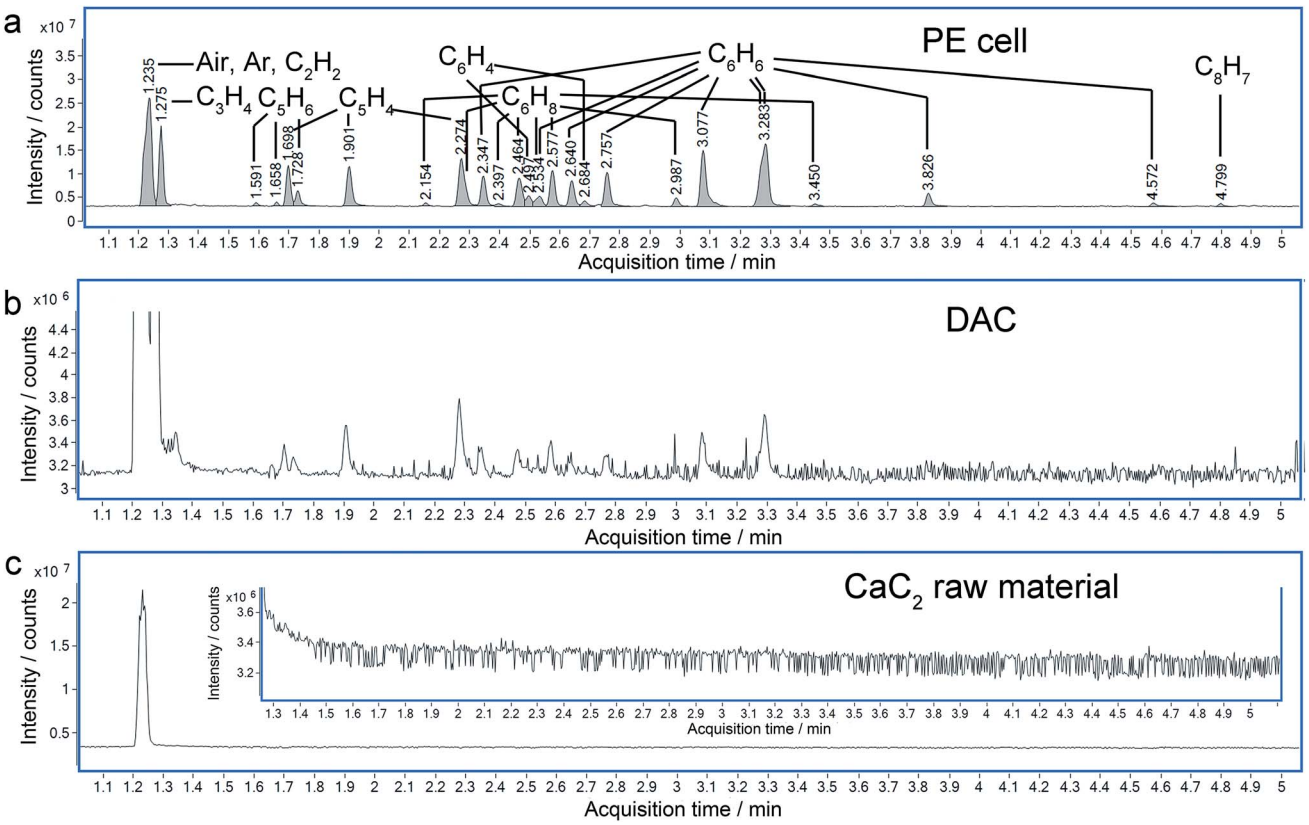


Fig. 7 Total ion chromatograms (TIC) of the product of $CaC_2$ recovered from 26 GPa and $CaC_2$ raw material reacting with water. (a) Sample synthesized by PE cell. (b) Sample synthesized by DAC. (c) $CaC_2$ raw material (before compression).

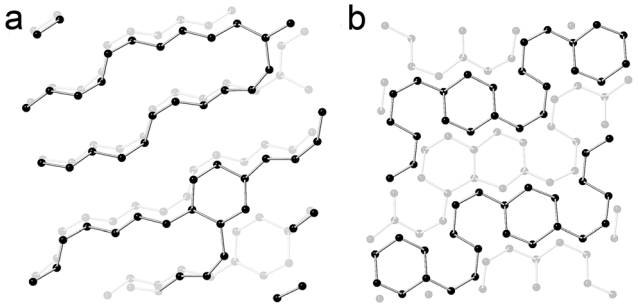


Fig. 8 Simulated structure of $CaC_2$ at 30 GPa by meta-dynamics. (a) Chain model. (b) Ribbon model. The C–C bond limitation is set at 1.6 Å. Ca ions are omitted for clarity.

### Decreased resistivity

One of the most attractive properties of the metal carbide materials is their electrical property, which is closely related to its structure.[7] In this work, the pressure dependent resistivity of $CaC_2$ was measured. From ~2 GPa to ~22 GPa, the resistivity decreases by seven orders of magnitude (Fig. 9), with a turning point at the minor transition around 10–12 GPa. From ~10 GPa to 22 GPa, the resistivity decreases by 1 order of magnitude, while below 10 GPa, it decreases by six orders. This significant decrease of resistivity ($R$) should be attributed to the decrease of both $R_g$ and $R_{gb}$, where $R_g$ and $R_{gb}$ stand for the resistance of grains and grain boundaries respectively. Because $R = R_g + R_{gb}$ and $R_g$ and $R_{gb}$ are usually in the same order of magnitude, for a $10^7$ fold decrease, both $R_g$ and $R_{gb}$ should decrease. The decrease of $R_g$ is most likely attributed to the narrowing of the band gap. The band gap of $CaC_2$-I decreases when compressed (Fig. S8†) and reaches 0 eV at ~18 GPa as indicated by the theoretical calculations (Fig. S9† by interpolation). The interaction between $C_2^{2-}$ units is enhanced when the C···C distance is decreased, which broadens the energy bands and reduces the band gap. Quantitatively, from the formula $\sigma = ne(\mu_- + \mu_+) = 2\sqrt{N_-N_+}e^{-\frac{E_g}{2kT}} \cdot e(\mu_- + \mu_+)$,[14] we can derive $\lg \rho = -\lg(2\sqrt{N_-N_+} \cdot e(\mu_- + \mu_+)) + \frac{E_g}{2kT} \cdot 0.4343 = -\lg(2\sqrt{N_-N_+} \cdot e(\mu_- + \mu_+)) + 8.46E_g$ ($E_g$ in eV), where $\rho$ and $\sigma$ are the resistivity and conductivity, $n$ is the concentration of electrons and holes, $N_-$ and $N_+$ are the density of states at the bottom of the conduction band and the top of the valence band, $\mu_-$ and $\mu_+$ are the carrier mobilities, $E_g$ is the band gap, $k$ is the Boltzmann constant, $T$ is the absolute temperature, and $e$ is the charge of an electron. From 2 GPa to 6 GPa, $\Delta E_g = 0.23$ eV, and the variation of the second term $\Delta(8.46E_g) = 2$, which is partly responsible for the decrease of lg $\rho$ (~4) (Table S2†). The other remainder of the decrease should be attributed to the enhancing of $N_-$, $N_+$, $\mu_+$, and/or $\mu_-$ in the first term, $-\lg(2\sqrt{N_-N_+} \cdot e(\mu_- + \mu_+))$, or other extrinsic reasons. In the view of real (direct) space, the decrease of $R$ can simply be attributed to the increasing overlap of the $\pi$ and $\pi^*$-orbitals, which enhances the mobilities ($\mu_-$ and $\mu_+$). This is similar to fused-ring molecules under high pressure.[15]

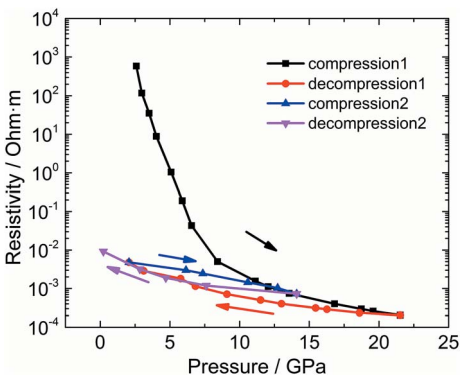


Fig. 9 Pressure dependent electrical resistivity of $CaC_2$.

The irreversibility of the resistance decrease is evidenced by the two compression loops. This irreversibility is most likely attributed to the covalent bonding between the acetylide anions. The transitions accompanied with the formation of covalent bonds are often (kinetically) stable, just like the transition from graphite to diamond. In this work we show it is also true for metal carbides in the experimental time scale. The high conductivity is also recovered, which suggests that this pressure induced polymerization can be used to prepare conductive metal polycarbide materials from insulating monomers.

It is also notable that the d-orbital of $Ca^{2+}$ also contributes to the valence band and the conduction band, as indicated by the theoretical calculations (shown in Fig. S8†). In compounds with the same structure, such as $UC_2$, U donates 6d electrons to $C_2$, forming a $C_2^{4-}$ anion, and $UC_2$ is metallic.[16] As such, the d–$\pi$ interaction acts as another important factor that may affect the conductivity. Additionally, it also suggests the possibility of introducing a transition metal for doping, which is always a promising method to improve the conductivity, as in polyacetylene.[17]

## Conclusions

In summary, the phase transitions of $CaC_2$ under external pressure were systematically investigated and the polymerization of $C_2^{2-}$ was confirmed using *in situ* XRD, neutron diffraction, Raman, IR and impedance spectra, as well as neutron PDF and GC-MS. The reaction in the amorphous $CaC_2$ was firstly probed. The polymerized product can be recovered to ambient pressure. Benzene and several other hydrocarbon molecules are identified in the hydrolyzed product of the recovered sample, which clearly evidences the formation of $C_6^{6-}$ and other polycarbide anions. Accompanied with the structural variations, the conductivity of $CaC_2$ was enhanced by more than $10^7$ fold, which demonstrates the dramatic effects of high pressure on the electrical properties of materials. The polymerization helps to stabilize the high conductivity at ambient pressure, and suggests the possibility to stabilize the predicted phases including calcium graphenide and calcium polyacetylide. This will have a great impact on the current research of functional metal-carbon materials, and more novel metal polycarbide materials can be expected from the high-pressure synthesis. In

addition, since these highly charged species like $C_6^{6-}$ are easy to be functionalized, this method can be further applied to synthesize more complicated Ca organics and other metallic organics.

## Acknowledgements

The authors acknowledge the support of NSAF (Grant No. U1530402) and NSFC (Grant No. 21501162). This work was supported as part of the Energy Frontier Research in Extreme Environment Center (Efree), an Energy Frontier Research Center funded by the U.S. Department of Energy, Office of Science, Basic Energy Sciences under Award DE-SC0001057. A portion of this research was performed at HPCAT (Sector 16), Advanced Photon Source (APS), Argonne National Laboratory. HPCAT (Geophysical Lab) operations are supported by DOE-NNSA under Award No. DE-NA0001974 and DOE-BES under Award No. DE-FG02-99ER45775, with partial instrumentation funding by NSF. APS is supported by DOE-BES, under Contract No. DE-AC02-06CH11357. A portion of this research was conducted at the Center for Nanophase Materials Sciences and Spallation Neutron Source, which are sponsored at Oak Ridge National Laboratory by the Scientific User Facilities Division, Office of Basic Energy Sciences, U.S. Department of Energy. The authors thank Dr Antonio F. Moreira dos Santos for the help in the neutron diffraction experiment, Dr Hongping Yan for the help in the *in situ* XRD experiment and Dr George Cody for valuable discussion. SNAP pressure cells were used to synthesize many of the *in situ* and *ex situ* samples used in this study. Work at IOPCAS was supported by NSF & MOST through research projects. The authors thank Agilent Technologies (China), Inc. for assistance in the GC-MS experiment. The metadynamic calculations were performed at Tianhe II in Guangzhou which is supported by Special Program for Applied Research on Super Computation of the NSFC-Guangdong Joint Fund (the second phase).

## References

1 P. Srepusharawoot, A. Blomqvist, C. Moysés Araújo, R. H. Scheicher and R. Ahuja, *Phys. Rev. B: Condens. Matter Mater. Phys.*, 2010, **82**, 125439.
2 X. Q. Chen, C. L. Fu and C. Franchini, *J. Phys.: Condens. Matter*, 2010, **22**, 292201.
3 I. Efthimiopoulos, K. Kunc, G. V. Vazhenim, E. Stavrou, K. Syassen, M. Hanfland, St. Liebig and U. Ruschewitz, *Phys. Rev. B: Condens. Matter Mater. Phys.*, 2012, **85**, 054105.
4 N.-G. Vannerberg, *Acta Chem. Scand.*, 1962, **16**, 1212–1220.
5 N.-G. Vannerberg, *Acta Chem. Scand.*, 1961, **15**, 769–774.
6 M. Knapp and U. Ruschewitz, *Chem.–Eur. J.*, 2001, **7**, 874–880.
7 Y. L. Li, W. Luo, Z. Zeng, H.-Q. Lin, H.-k. Mao and R. Ahuja, *Proc. Natl. Acad. Sci. U. S. A.*, 2013, **110**, 9289–9294.
8 A. Kulkarni, K. Doll, J. C. Schon and M. Jansen, *J. Phys. Chem. B*, 2010, **114**, 15573–15581.
9 D. Benson, Y. Li, W. Luo, R. Ahuja, G. Svensson and U. Häussermann, *Inorg. Chem.*, 2013, **52**, 6402–6406.
10 J. Nylen, S. Konar, P. Lazor, D. Benson and U. Haussermann, *J. Chem. Phys.*, 2012, **137**, 224507.
11 I. Efthimiopoulos, G. V. Vajenine, E. Stavrou, K. Syassen, St. Liebig, U. Ruschewitz and M. Hanfland, *Acta Crystallogr.*, 2010, **66**, s197.
12 L. Wang, X. Huang, D. Li, Y. Huang, K. Bao, F. Li, G. Wu, B. Liu and T. Cui, *J. Chem. Phys.*, 2016, **144**, 194506.
13 S. J. L. Billinge and M. G. Kanatzidis, *Chem. Commun.*, 2004, 749–760.
14 K. Huang and R. Han, *Solid State Physics*, Higher Education Press, Beijing, 1st edn, 1988.
15 G. A. Samara and H. G. Drickamer, *J. Chem. Phys.*, 1962, **37**, 474–479.
16 J. Li and R. Hoffmann, *Chem. Mater.*, 1989, **1**, 83–101.
17 H. Shirakawa, E. J. Louis, A. G. Macdiarmid, C. K. Chiang and A. J. Heeger, *J. Chem. Soc., Chem. Commun.*, 1977, **16**, 578–580.